Journal of the Physical Society of Japan
Vol. 54, No. 5, May, 1985, pp. 1757–1768

Differential Cross Sections of Electron Scattering from Molecular Hydrogen I. Elastic Scattering and Vibrational Excitation ($X^1\Sigma_g^+, v=0\rightarrow1$)

Hiroyuki NISHIMURA, Atsunori DANJO and Hiroshi SUGAHARA*

Department of Physics, Niigata University, Niigata 950-21

(Received January 11, 1985)

Differential cross sections (DCS's) for the elastic scattering and the vibrational excitation of molecular hydrogen by electron impact have been measured in the energy range from 2.5 eV to 200 eV and in the angular range from 10° to 120°. Absolute values of the DCS's are obtained by normalizing the relative values to the absolute elastic DCS's for He by means of the relative flow method. Integral and momentum transfer cross sections for each scattering process are also given. Differential, integral and momentum transfer cross sections obtained in the present measurements are compared with the previous experimental and theoretical results.

§1. Introduction

Electron-molecular hydrogen collision is the simplest process in the electron-molecule collisions. Through this process, much theoretical and experimental effort has been done for testing physical models and for understanding transportation phenomena and energy deposition of electrons in gaseous discharge, high temperature plasma, planetary and earth's upper atmosphere. In the low energy region (below the excitation threshold), the elastic scattering is a dominant process in the electron-molecule collisions. From this point of view, the total cross sections are used as a standard for the normalization of the measured elastic cross sections. The total cross sections measured by Golden *et al.*[1] have been referred as a standard by several authors. The swarm experiments have provided the momentum transfer cross sections at very low electron energy region where an electron beam experiment is very difficult. The results in such energy region were reported by Crompton *et al.*[2] and Engelhardt and Phelps.[3] Among the theoretical calculations, the elastic DCS's by Hara,[4] Henry and Lane,[5] Truhlar and Brandt,[6] and Burke[7] gave good predictions for the experimental results of Linder and Schmidt,[8] and Trajmar *et al.*[9] In the high energy region (above about ten times of the ionization potential), the calculated DCS's by Khare and Shobha,[10] Gupta and Khare,[11] and Bhattacharyya *et al.*[12] are in good agreement with the measurements of Fink *et al.*[13] and van Wingerden *et al.*[14]

However, in the intermediate energy region there are few theoretical calculations which predict the experimental DCS's. Furthermore, the experimental works thus far reported are very few in this energy region. Both experimentally and theoretically, there is very few information available on the inelastic scattering including the ground state vibrational excitations. The theoretical and experimental works were reviewed by Golden *et al.*,[15] Lane[16] and Trajmar *et al.*[17]

Thus far, the elastic DCS's have been measured by Linder and Schmidt (0.6–10.8 eV, 20°–120°),[8] Lloyd *et al.* (9.4–200 eV, 15°–135°),[18] Srivastava *et al.* (3–75 eV, 20°–135°),[19] Shyn and Sharp (2–200 eV, −96°–156°)[20] and Frust *et al.* (1–19 eV, 20°–115°)[21] using the crossed beam technique. Linder and Schmidt normalized their relative DCS's to the total cross section of Golden *et al.*[1] Srivastava *et al.*[20] put an absolute scale on their values

* Present address: Ushio Electric Inc., Himeji 671-02.

with the relative flow method, which was developed by themselves, by normalizing to the elastic DCS's for He reported by McConkey and Preston.[22] Recently they have reported the renormalized DCS's referring the new elastic e-He DCS's given by Register *et al.*[23] Shyn and Sharp[21] normalized their relative values to the theoretical elastic DCS's for He given by LaBahn and Callaway[24] at the electron energy of 10 eV. The measurements of Frust *et al.* are normalized to their own absolute elastic cross sections for He.[25] The DCS's for vibrational excitations have been measured by Ehrhardt *et al.* (1–10 eV),[26] Trajmar *et al.* (7–81.6 eV),[27] and Linder and Schmidt (3–13 eV, 20°–120°).[8]

The DCS's for the elastic scattering, vibrational excitations and electronic excitations in e-H_2 collision have been measured precisely over the wide energy range. The elastic DCS's are fundamentally important because the absolute values of the DCS's for the inelastic scatterings are determined referring these values. One of the aims of the present measurements is to confirm the validity of the relative flow method for the determination of the absolute DCS's and to extend the results of Srivastava *et al.*, which were obtained with the same normalization technique. As an onset of our series, the DCS's for the elastic scattering and the vibrational excitation are reported in the electron energy range from 2.5 to 200 eV and in the angular range from 10° to 120°. The DCS's and integral cross sections are compared with the experimental and theoretical results.

The vibrational DCS's determined referring the elastic DCS's obtained in this work are compared with the experimental results of Trajmar *et al.*, Linder and Schmidt, and the calculated results of Chang *et al.*,[28] and Klonover and Kaldor (ab initio calculation).[29] The integral cross sections derived from the DCS's are also compared with the experimental results of Ehrhardt *et al.*, Crompton *et al.*, Linder and Schmidt, and with the calculated results of Henry and Chang,[30] Chang *et al.*, and Klonover and Kaldor.

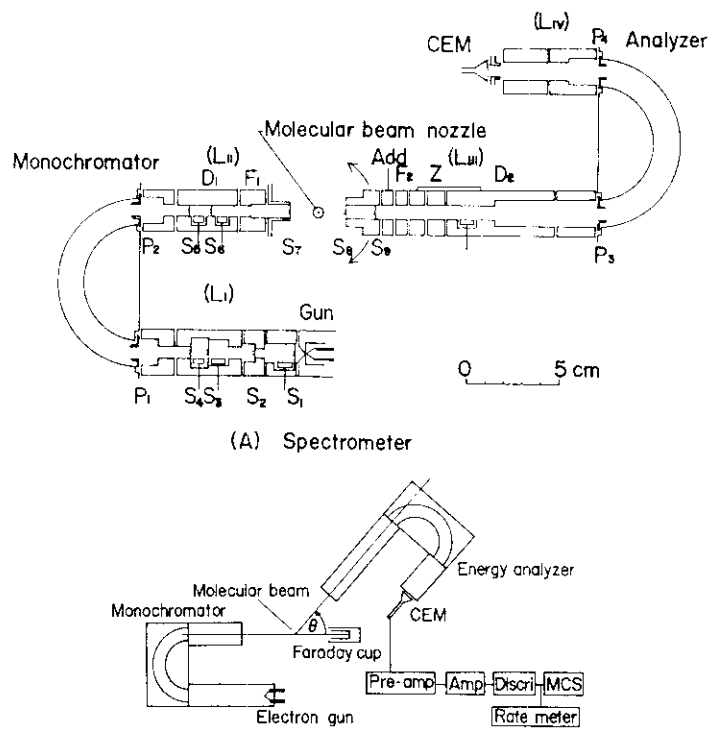

Fig. 1. Schematic diagram of the experimental apparatus.

§2. Experimental

2.1 Apparatus

An electron spectrometer used in the present measurements is arranged in a crossed beam type as shown in Fig. 1. It consists of an electron gun, a cylindrical lens system (LI, LII, LIII, LIV), a hemispherical electrostatic monochromator, a same type of analyzer, an electron detector (Murata, EMT 6081B), a Faraday cup and a molecular beam source. The electron optics are similar to those designed by Chutjian[31] along with the principles outlined by Kuyatt *et al.*[32] The details of the design and its operation are discussed by Chutjian[31] and Jensen.[33]

Electrons from a hair pin tungusten filament of the Pierce type gun are accelerated and focused onto the slit S_3. The electrons at S_3 are then decelerated by the rear part of LI and focused at the entrance plane P_1 of the monochromator. The image at P_1 are focused through the monochromator onto the exit plane P_2 with 1 magnification. The electrons at P_2 are accelerated and focused at S_6, and finally focused onto the molecular beam by the lens LII. Appropriate voltage could be supplied on the element F_1 to ensure the image size and position at the target beam were independent of the final electron energy. Intensity and the angular spread of the electron beam are measured by a rotatable Faraday cup. Typical electron currents are 0.1 to 10 nA in the impact energy range from several eV to 200 eV. The scattered electrons from the molecular beam are collimated by the slits S_8 and S_9, and are then focused onto the entrance plane P_3 of the analyzer through LIII. To maintain the constant transmittance of the scattered electrons through LIII, the energy lost in the inelastic scattering is compensated by the potential supplied on the element Add. The voltage on the element F_2 is swept as a function of the loss energy of the scattered electrons to keep a fixed image diameter and position at P_3. The elements Z and D_2 compose a zoom lens for wide electron energy range. Energy analyzed electrons are focused into the cone of the channel electron multiplier by means of LIV. The pulses from the detector are amplified and accumulated in a multichannel analyzer (IT-5300) in MCS mode.

Elements of the spectrometer are made of gold plated nonmagnetic Cu–Ni alloy except for the gun and slits. All slits are made of molybdenum plate with appropriate circular apertures. The molecular beam is collimated (1 mm in diameter) after being effused through a multichannel glass capillary array (Hamamatsu Photonics) at the rotational center of the spectrometer. Magnetic field in the region of the spectrometer is reduced to about 10 mG or less by a three dimentional Helmholtz coil and a mu-metal can. The vacuum chamber is evacuated by a 10 in. oil diffusion pump with a liquid N_2 trap. The base pressure in the chamber is attained to several $\times 10^{-8}$ Torr. The background pressure in the chamber is kept $\sim 8\times 10^{-7}$ Torr in the elastic DCS's measurements and $\sim 5\times 10^{-6}$ Torr in the vibrational DCS's measurements. During the measurements, the spectrometer is baked to about 100°C by a small halogen lamp.

The electron analyzer system can be rotated around the center of the spectrometer in the angular range from $-15°$ to 120°. The energy loss spectra from H_2 are taken with an overall resolution of 80 meV. Due to the relatively poor resolution, the rotational excitations are not separated in the present measurements.

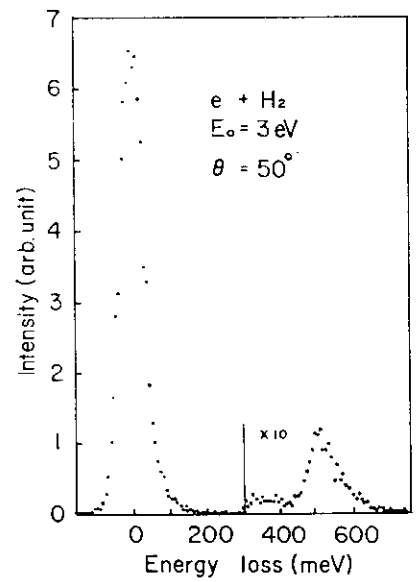

Fig. 2. Energy loss spectrum of H_2 at the impact energy of 3 eV and at the scattering angle of 50°. The elastic peak ($\Delta E=0$ eV) and the first vibrational excitation peak ($\Delta E=0.516$ eV) are shown.

A typical electron energy loss spectrum from H_2 at an electron energy of 3 eV and at a scattering angle of 50° is shown in Fig. 2, which shows an elastic peak and a first vibrational excitation peak ($X^1\Sigma_g^+, v=0\rightarrow1$). The scattered electron intensities are obtained by integrating the area under the peaks for the elastic scattering and the vibrational excitation. The transmittance of the electrons through LIII is assumed to be constant for elastically scattered electrons and for the electrons of the vibrational scattering with the following reasons. The lost energy of the electrons during the vibrational excitation is very small as compared with the incident electron energy because $v=1$ state lies at 0.516 eV above the $v=0$ state. Therefore, both electrons, elastically and vibrationally scattered, have almost the same kinetic energy. For the calibration of the impact electron energy, the elastic resonance scattering of He is used.

2.2 Normalization

The relative flow method is employed for the normalization of the elastic DCS's for H_2 using the elastic DCS's for He as a secondary standard. The theoretical background of the method has been discussed in detail by Srivastaba *et al.*[19] The outline of the procedure is as follows. The elastically scattered electron intensity $N_e(H_2, \theta)$ from H_2 is measured at a respective scattering angle θ and recorded. Soon after, H_2 gas is evacuated quickly and He gas is introduced. The electron intensity N_e(He, θ) from He is also measured at the same angle. Both the measurements have to be performed under as much the same conditions as possible. When the molecular flow through the capillary array is under the condition $\lambda/D>1$, the ratio of the cross sections for elastic scattering is related to the ratio of the two intensities;

$$\sigma(H_2, \theta)/\sigma(\mathrm{He}, \theta)=[N_e(H_2, \theta)/N_e(\mathrm{He}, \theta)][m(H_2)/m(\mathrm{He})]^{1/2}[N_b(\mathrm{He})/N_b(H_2)]$$
$$=[N_e(H_2, \theta)/N_e(\mathrm{He}, \theta)][p(\mathrm{He})/p(H_2)], \quad (1)$$

where λ is the mean free path of the molecule in the capillary array and D is the diameter of the capillary (12 micron). $N_e(H_2, \theta)$ and N_e(He, θ) are the rates of the elastically scattered electron intensities at angle θ. $N_b(H_2)$ and N_b(He) are the gas flow rates through the capillary array and $m(H_2)$ and m(He) are the molecular weight of each gas. The pressures of the gas behind the capillary array $p(H_2)$ and p(He) are measured by an oil manometer. The absolute values of $\sigma(H_2, \theta)$ are obtained from eq. (1) using the absolute values of σ(He, θ). As for the standard DCS's for He the experimental results of Register *et al.*[23] is adopted.

At a fixed impact energy, the energy loss spectrum is measured several times at each scattering angle. Through the measurements, the pressure at the back of the capillary array and the incident electron current are kept constant and monitored with an accuracy of 2%. In replacing H_2 by He, there is a small change of the primary electron current especially at low impact energies. Small corrections for the counting rates are made against these changes. Spurious background electrons are negligibly small except at low impact energies and small scattering angles. The genuine scattered electron intensities by H_2 and He are obtained by subtracting the background electron intensities measured with the molecular beam off at the corresponding scattering angles. In the replacement of the gases a small variation of the electron beam direction (<0.5°), and hence the changes of the collision volumes and the ambiguities in scattering angle measurements cause another error in the DCS's determinations. This uncertainty is estimated about 10% at small angles (<20°) and high impact energies. The statistical uncertainties are less than 3% except for large angles at high energies where the uncertainties are 5% for the elastic scattering and 7% for the vibrational excitation. The resultant values of the measured DCS's are well reproducible within 10% for several repetitions of measurements. Taking into account the accuracy of the standard elastic DCS's for He the overall uncertainty of the present elastic DCS's is less than 15% at the scattering angles larger than 20°. At the smaller angles below 20° it is estimated to be 20%.

Table I. Differential cross sections (cm^2/sr). Elastic scattering.

Angle (deg)	Energy (eV) 2.5 Expt.	2.5 Fit.	3.0 Expt.	3.0 Fit.	4.0 Expt.	4.0 Fit.	6.0 Expt.	6.0 Fit.
0		2.92-16*		3.77-16		4.12-16		4.29-16
10		2.72-16		3.07-16		3.64-16		3.52-16
20	2.63-16	2.44-16	2.36-16	2.50-16	3.36-16	3.08-16	2.71-16	2.89-16
25	2.41-16		2.10-16					
30	2.11-16	2.11-16	1.96-16	2.03-16	2.44-16	2.50-16	2.30-16	2.37-16
40	1.74-16	1.77-16	1.52-16	1.64-16	2.05-16	1.96-16	1.95-16	1.95-16
50	1.36-16	1.46-16	1.24-16	1.33-16	1.60-16	1.49-16	1.64-16	1.60-16
60	1.04-16	1.20-16	1.15-16	1.08-16	1.17-16	1.15-16	1.30-16	1.31-16
70	1.03-16	1.03-16	9.24-17	9.08-17	9.39-17	9.30-17	1.12-16	1.08-16
80	1.08-16	9.41-17	9.18-17	8.10-17	8.95-17	8.33-17	9.55-17	9.09-17
90	1.04-16	9.37-17	8.48-17	7.92-17	9.24-17	8.33-17	7.61-17	8.00-17
100	1.12-16	1.00-16	8.47-17	8.58-17	8.86-17	8.98-17	6.36-17	7.52-17
110	1.02-16	1.12-16	9.86-17	1.00-16	9.86-17	9.97-17	7.24-17	7.65-17
120	1.14-16	1.27-16	1.09-16	1.22-16	1.23-16	1.10-16	8.04-17	8.32-17
130		1.43-16		1.49-16		1.20-16		9.40-17
140		1.58-16		1.74-16		1.27-16		1.07-16
150		1.70-16		2.05-16		1.32-16		1.21-16
160		1.80-16		2.28-16		1.35-16		1.33-16
170		1.86-16		2.43-16		1.37-16		1.41-16
180		1.88-16		2.48-16		1.37-16		1.43-16
σ_I (cm^2)		1.71-15		1.68-15		1.62-15		1.54-15
σ_M (cm^2)		1.65-15		1.68-15		1.41-15		1.27-15

(continued)

Angle (deg)	Energy (eV) 8.0 Expt.	8.0 Fit.	10.0 Expt.	10.0 Fit.	15.0 Expt.	15.0 Fit.	20.0 Expt.	20.0 Fit.
0		6.14-16		5.14-16		6.03-16		5.63-16
10		4.41-16		3.87-16		4.14-16	3.11-16	3.74-16
15	5.70-16		3.45-16		2.94-16		2.88-16	
20	3.20-16	3.19-16	2.53-16	2.89-16	2.85-16	2.84-16	2.35-16	2.47-16
30	2.31-16	2.35-16	2.02-16	2.15-16	1.98-16	1.95-16	1.54-16	1.63-16
40	1.73-16	1.77-16	1.65-16	1.59-16	1.30-16	1.33-16	1.04-16	1.09-16
50	1.34-16	1.37-16	1.15-16	1.19-16	9.39-17	9.00-17	6.75-17	7.22-17
60	1.03-16	1.09-16	8.13-17	9.09-17	6.32-17	6.05-17	4.87-17	4.78-17
70	9.15-17	8.79-17	7.38-17	7.12-17	4.51-17	4.10-17	3.35-17	3.14-17
80	6.88-17	7.26-17	5.48-17	5.78-17	3.49-17	2.87-17	2.13-17	2.09-17
90	5.86-17	6.16-17	4.70-17	4.89-17	2.30-17	2.13-17	1.70-17	1.45-17
100	5.54-17	5.40-17	3.77-17	4.32-17	1.87-17	1.71-17	1.15-17	1.11-17
110	4.66-17	5.00-17	3.89-17	3.96-17	1.48-17	1.49-17	9.95-18	9.70-18
120	4.64-17	4.82-17	3.94-17	3.75-17	1.37-17	1.40-17	8.24-18	9.48-18
130		4.92-17		3.62-17		1.43-17		9.79-18
140		5.20-17		3.55-17		1.56-17		1.03-17
150		5.56-17		3.51-17		1.78-17		1.07-17
160		5.92-17		3.48-17		2.03-17		1.09-17
170		6.18-17		3.47-17		2.22-17		1.11-17
180		6.27-17		3.47-17		2.29-17		1.11-17
σ_I (cm^2)		1.22-15		1.01-15		7.17-16		5.74-16
σ_M (cm^2)		8.03-16		6.14-16		3.20-16		2.27-16

(continued)

Angle (deg)	Energy (eV) 25.0		30.0		40.0		50.0	
	Expt.	Fit.	Expt.	Fit.	Expt.	Fit.	Expt.	Fit.
0		4.96-16		5.18-16		5.24-16		3.98-16
10	2.83-16	3.21-16	3.07-16	3.07-16	2.55-16	2.51-16	1.97-16	1.97-16
15	2.34-16							
20	1.89-16	2.03-16	1.81-16	1.76-16	1.11-16	1.22-16	9.81-17	9.41-17
30	1.25-16	1.26-16	9.17-17	9.83-17	6.68-17	6.39-17	4.98-17	4.52-17
40	7.82-17	7.84-17	5.14-17	5.52-17	3.62-17	3.65-17	2.33-17	2.30-17
50	4.75-17	4.92-17	2.85-17	3.24-17	2.08-17	2.18-17	1.31-17	1.28-17
60	2.96-17	3.17-17	2.05-17	1.99-17	1.31-17	1.31-17	8.41-18	7.83-18
70	2.04-17	2.14-17	1.20-17	1.33-17	6.96-18	7.97-18	4.88-18	5.16-18
80	1.42-17	1.51-17	8.69-18	9.44-18	5.32-18	5.13-18	3.68-18	3.61-18
90	1.03-17	1.13-17	6.90-18	7.04-18	3.59-18	3.62-18	2.60-18	2.64-18
100	8.55-18	8.91-18	4.78-18	5.46-18	2.54-18	2.82-18	1.93-18	2.01-18
110	7.01-18	7.35-18	4.01-18	4.38-18	2.35-18	2.36-18	1.62-18	1.59-18
120	6.05-18	6.34-18	3.45-18	3.65-18	1.98-18	2.04-18	1.55-18	1.35-18
130		5.69-18		3.17-18		1.78-18		1.24-18
140		5.29-18		2.91-18		1.59-18		1.21-18
150		5.06-18		2.83-18		1.53-18		1.20-18
160		4.95-18		2.87-18		1.60-18		1.20-18
170		4.90-18		2.94-18		1.75-18		1.19-18
180		4.88-18		2.97-18		1.82-18		1.18-18
σ_I (cm^2)		4.29-16		3.25-16		2.23-16		1.59-16
σ_M (cm^2)		1.54-16		9.78-17		5.85-17		3.95-17

(continued)

Angle (deg)	Energy (eV) 60.0		70.0		80.0		90.0	
	Expt.	Fit.	Expt.	Fit.	Expt.	Fit.	Expt.	Fit.
0		4.41-16		4.07-16		3.20-16		3.61-16
10	1.77-16	1.77-16	1.67-16	1.67-16	1.32-16	1.32-16	1.38-16	1.38-16
20	8.36-17	7.13-17	6.63-17	6.76-17	5.77-17	5.17-17	5.19-17	5.00-17
30	3.79-17	3.35-17	3.24-17	3.01-17	2.67-17	2.15-17	2.21-17	1.99-17
40	2.04-17	1.88-17	1.61-17	1.56-17	1.23-17	1.04-17	1.07-17	9.50-18
50	1.03-17	1.12-17	8.46-18	8.87-18	5.94-18	5.69-18	5.08-18	5.05-18
60	5.90-18	6.56-18	4.49-18	5.25-18	3.30-18	3.37-18	2.93-18	2.80-18
70	4.05-18	3.93-18	3.30-18	3.24-18	2.00-18	2.18-18	1.93-18	1.73-18
80	2.55-18	2.53-18	2.04-18	2.15-18	1.30-18	1.59-18	1.17-18	1.26-18
90	1.97-18	1.78-18	1.62-18	1.58-18	1.06-18	1.27-18	9.86-19	1.05-18
100	1.32-18	1.38-18	1.20-18	1.33-18	9.95-19	1.07-18	9.32-19	9.00-19
110	1.25-18	1.17-18	1.29-18	1.25-18	9.02-19	9.20-19	6.99-19	7.70-19
120	1.22-18	1.08-18	1.24-18	1.15-18	8.15-19	8.30-19	6.50-19	6.70-19
130		9.80-19		1.10-18		7.50-19		5.90-19
140		9.20-19		1.05-18		6.80-19		5.30-19
150		8.80-19		1.02-18		6.30-19		4.80-19
160		8.60-19		1.00-18		5.90-19		4.50-19
170		8.60-19		9.80-19		5.70-19		4.20-19
180		8.70-19		9.80-19		5.60-19		4.05-19
σ_I (cm^2)		1.35-16		1.15-16		8.66-17		8.26-17
σ_M (cm^2)		3.22-17		2.80-17		1.95-17		1.70-17

(continued)

Angle (deg)	Energy (eV) 100.0 Expt.	100.0 Fit.	150.0 Expt.	150.0 Fit.	200.0 Expt.	200.0 Fit.
0		2.77-16		1.36-16		1.24-16
10	1.11-16	1.09-16	6.26-17	6.26-17	5.31-17	5.31-17
20	3.74-17	4.01-17	2.49-17	2.68-17	2.02-17	2.08-17
30	1.76-17	1.55-17	1.24-17	1.11-17	6.32-18	7.82-18
40	7.58-18	6.97-18	4.56-18	4.82-18	2.74-18	3.05-18
50	3.50-18	3.58-18	2.37-18	2.39-18	1.28-18	1.37-18
60	2.07-18	2.05-18	1.50-18	1.39-18	7.73-19	7.41-19
70	1.32-18	1.34-18	8.68-19	9.20-19	4.96-19	4.53-19
80	1.02-18	1.01-18	6.50-19	6.80-19	2.84-19	2.97-19
90	8.29-19	8.30-19	5.32-19	5.30-19	2.00-19	2.11-19
100	6.77-19	7.00-19	4.48-19	4.30-19		1.62-19
110	5.82-19	6.00-19	3.22-19	3.50-19		1.31-19
120	5.14-19	5.30-19	3.00-19	2.90-19		1.10-19
130		4.75-19		2.50-19		1.01-19
140		4.40-19		2.30-19		9.00-20
150		4.00-19		2.10-19		8.30-20
160		3.80-19		2.10-19		8.00-20
170		3.55-19		2.00-19		7.70-20
180		3.30-19		2.00-19		7.70-20
σ_I (cm^2)		6.48-17		4.09-17		2.98-17
σ_M (cm^2)		1.27-17		8.12-18		4.25-18

* 2.92-16 = 2.92×10^{-16}.

The DCS's for vibrational excitation are determined within 20% uncertainty.

§3. Results and Discussion

3.1 Elastic scattering cross sections

The absolute differential cross sections for elastic scattering from H_2 are summarized in Table I. In the present experiments, measurements were done only in the angular range up to 120°. To obtain the integral and momentum transfer cross sections, the DCS's have to be extrapolated to experimentally inaccesible angles. A phase shift analysis is usually done for electron atom scattering below first inelastic threshold. In the present measurements, a modified phase shift analysis was used just for purposes of exprapolation. The details of the fitting procedures are discussed by Register *et al.*[23] The fitted and extrapolated values are also listed in Table I. The integral and momentum transfer cross sections are calculated with these values and given at the bottom of each column. Figures 3, 4 and 5 show typical angular dependences of the elastic DCS's at low, intermediate and high impact energies, respectively.

In Fig. 3, the present results at 10 eV are plotted together with the experimental results of Linder and Shmidt,[8] Srivastava *et al.*,[19] Shyn and Sharp,[20] Frust *et al.*,[21] and the results of two center calculations of Hara[5] and the close-coupling calculations of Truhlar and Brandt There is a good agreement between the present results and those of Shyn and Sharp. The present results are also in good agreement with the results of Linder and Schmidt and those of Frust *et al.* in the forward direction. However, both the measurements give smaller values than the present results in the backward scattering. The results of Srivastava *et al.* are slightly smaller than the present results both in forward and backward directions. The calculations of Hara is in excellent agreement with the present results not only in shape but also in magnitude.

In Fig. 4 the present results at 40 eV are compared with other experimental[19,20] and theoretical results.[6,7,12] The present results are again in good agreement with the measurements of Shyn and Sharp although the

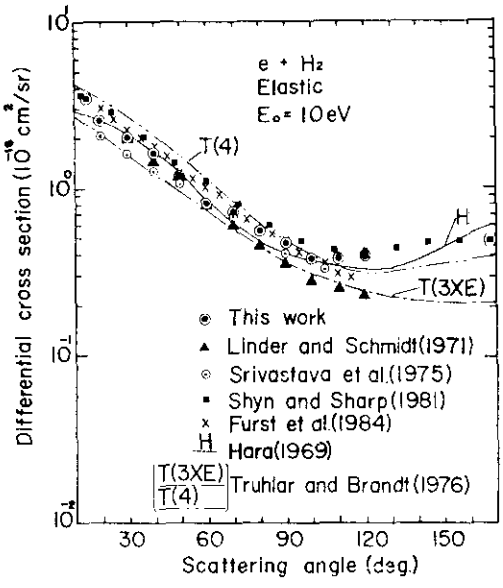

Fig. 3. Differential cross section for elastic scattering as a function of scattering angle at 10 eV. Experimental results of Linder and Schmidt shown here are the sum of the pure elastic scattering ($\Delta v = 0$, $\Delta j = 0$) and rotational excitation ($\Delta v = 0$, $j = 1 \rightarrow 3$). The curves marked T(3XE) and T(4) are the calculated results of Truhlar and Brandt for model potentials 3XE and 4 including rotational excitations.

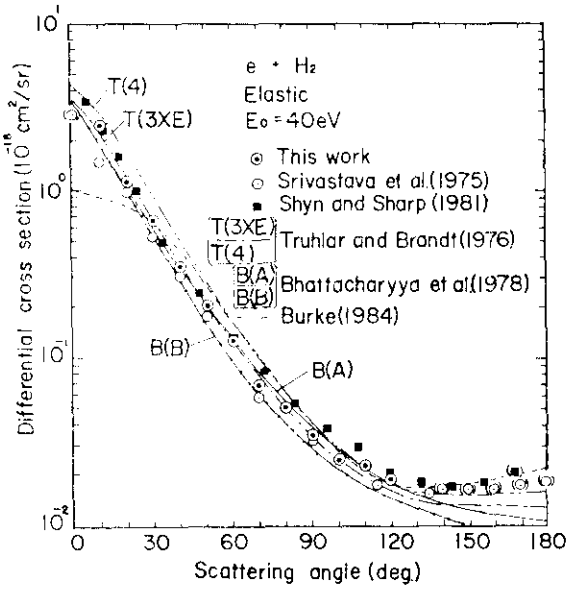

Fig. 4. Differential cross section for elastic scattering as a function of scattering angle at 40 eV. The solid lines B(A) and B(B) are the model A and model B calculations of Bhattacharyya *et al.*

present values are slightly low at the scattering angles from 70° to 110°. The calculations of Truhlar and Brandt reproduce the present results very well. The calculations of an adiabatic approximation by Bhattacharyya *et al.* also give excellent predictions of the present results except in the backward scattering. The experimental results are well interpreted by the two potential theory of Burke with the exception of the underestimates in the forward scattering.

Figure 5 shows the present results at 100 eV with the previous experimental results of Fink *et al.*,[13] van Wingerden *et al.*,[14] and Shyn and Sharp. Also are shown the theoretical results of the plane wave approximation including exchange and polarization by Khare and Shobha,[10] and the calculations of Bhattacharyya *et al.* The present results are about 16% lower on an average than those of Shyn and Sharp in the scattering angles below 90° with a better agreement at larger angles. The present results are well reproduced by the calculations of Khare and Shobha except at the intermediate scattering angles, where their calculations are slightly larger than the present results.

The integral cross sections are shown in Fig. 6 along with the experimental[8,13,14,19-21] and theoretical results.[10-12] The present

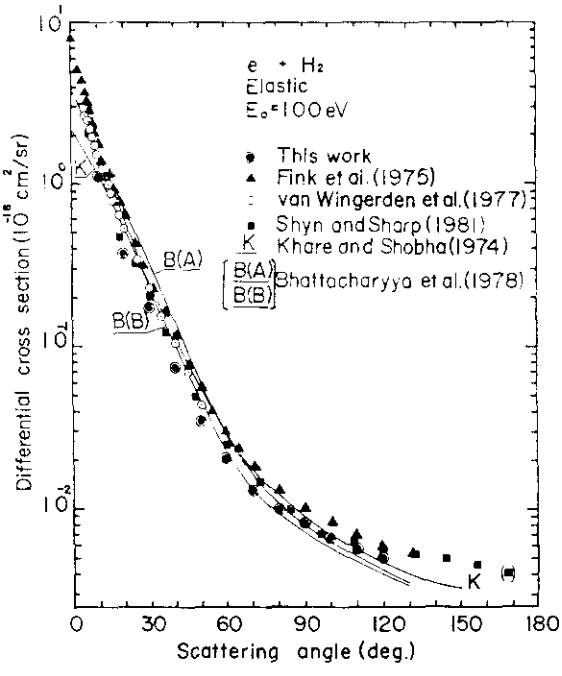

Fig. 5. Differential cross section for elastic scattering as a function of scattering angle at 100 eV. The symbols are same as Fig. 4.

results agree very well with the results of Shyn and Sharp from the lowest impact electron energy to 100 eV. However, above 100 eV the present results decrease more rapidly with energy than the previous results. There is an excellent agreement between the calculations of Hara and the present data at low energies. The calculations of Khare and Shobha give good predictions of the present experimental results at high impact energies (>60 eV). The first Born approximation (FBA) by Gupta and Khare gives lower cross section than the present measurements by a factor of 2 at 150 eV. The calculations of Bhattacharyya *et al.* give good predictions of the experimental results only in the intermediate energy region.

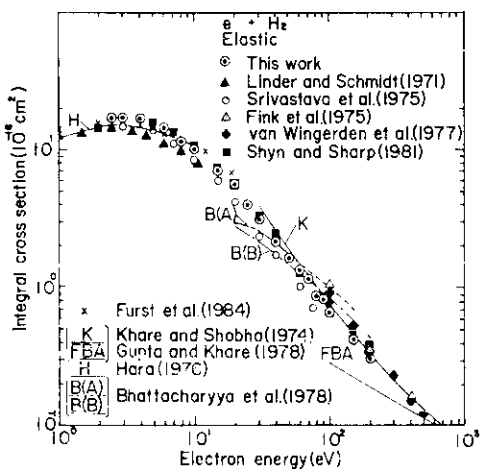

Fig. 6. Integral cross sections for elastic scattering as a function of impact energy. The solid line K is the calculated results of Khare and Shobha by the plane wave approximation including polarization and exchange. The solid line marked FBA is presented by integrating the DCS's of first Born approximation (ref. 11).

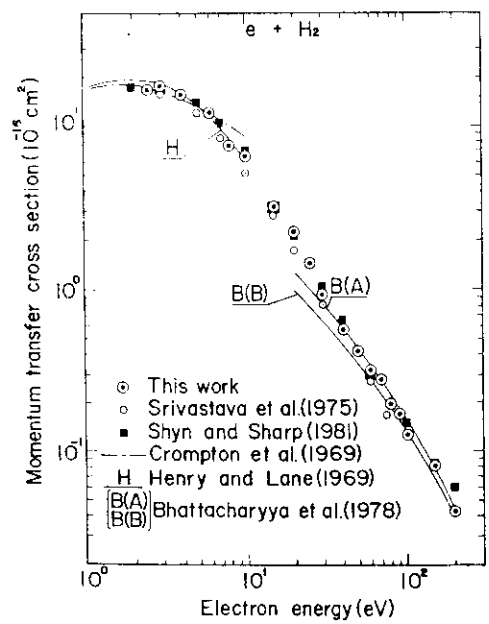

Fig. 7. Momentum transfer cross sections for elastic scattering as a function of impact energy.

The momentum transfer cross sections obtained in the present measurements are shown in Fig. 7 with the results of Srivastava *et al.*, Shyn and Sharp, and Crompton *et al.*[2] The calculations of Henry and Lane,[4] and Bhattacharyya *et al.* are also shown in the figure. All the experimental results are in good agreement in the entire region of impact energies. The present results are well reproduced by the theoretical results of Henry and Lane in the lower energy region, and in the higher region by the calculation of Bhattacharyya *et al.*

3.2 Vibrational excitation

The ratio of the differential cross sections for excitation of the first vibrational state ($X^1\Sigma_g^+$, $v=0\rightarrow1$) to the elastic DCS's have been measured as a function of the scattering angles in the 10°–120° range and energy range of 2.5 eV–100 eV. From these ratios the vibrational DCS's are obtained by using the present elastic cross sections.

The DCS's for the vibrational excitation are given in Table II. The integral cross sections are calculated from these DCS's and given at the bottom of each column. The measured DCS's are extrapolated to forward and backward directions with the procedures employed in the case of the elastic DCS's or by an eye fitting for the determination of the integral cross sections.

The angular distribution of the vibrational DCS's at low electron energies (<10 eV) show a symmetrical shape with a shallow bottom at around 90°. This type of angular behaviour is predicted by resonance theories for scattering by means of an intermediate negative ion state $H_2^-(^2\Sigma_u^+)$.[26,34,35] As the impact energy increases, the bottom becomes deeper and moves towards the smaller scattering angle and another kind of angular behaviour can be seen at above 20 eV. The angular distribution at high impact energies has a characteristic

Table II. Differential cross sections (cm^2/sr). Vibrational excitation.

Angle (deg)	Energy (eV) 2.5	3.0	4.0	6.0	8.0	10.0	15.0	20.0
15						2.13-18*	9.99-19	
20	5.59-18	6.20-18	6.99-18	3.51-18	2.99-18	1.70-18	8.07-19	5.18-19
25	5.47-18	5.64-18						
30	5.07-18	5.48-18	6.25-18	3.23-18	2.31-18	1.41-18	5.07-19	2.17-19
40	4.15-18	4.01-18	5.50-18	2.93-18	1.87-18	1.19-18	3.26-19	1.41-19
50	3.21-18	3.24-18	4.06-18	2.32-18	1.54-18	9.50-19	2.08-19	1.24-19
60	3.07-18	3.16-18	3.71-18	1.88-18	1.30-18	6.82-19	1.67-19	1.04-19
70	2.82-18	2.40-18	2.92-18	1.68-18	1.18-18	6.76-19	1.47-19	1.17-19
80	2.92-18	2.31-18	2.53-18	1.56-18	1.09-18	5.26-19	1.94-19	1.35-19
90	2.82-18	2.10-18	2.67-18	1.39-18	1.02-18	6.39-19	2.21-19	1.68-19
100	2.90-18	2.13-18	2.54-18	1.46-18	1.17-18	6.99-19	3.08-19	2.01-19
110	3.06-18	2.64-18	2.74-18	2.11-18	1.26-18	1.01-18	4.42-19	2.70-19
120	3.34-18	2.92-18	3.04-18	3.39-18	1.64-18	1.50-18	5.40-19	3.22-19
σ_I (cm^2)	4.50-17	4.79-17	4.62-17	3.69-17	2.04-17	1.52-17	5.65-18	3.32-18

(continued)

Angle (deg)	Energy (eV) 25.0	30.0	40.0	50.0	60.0	80.0	100.0
10	1.08-18		7.26-19		3.50-19	2.49-19	1.67-19
15	6.69-19	5.23-19	2.54-19	1.95-19	1.13-19		
20	3.33-19	2.54-19	4.86-20	7.30-20	6.48-20	4.81-20	3.72-20
30	1.12-19	7.27-20	5.47-20	5.37-20	7.18-20	6.25-20	4.52-20
40	7.38-20	7.28-20	8.04-20	7.56-20	8.44-20	7.71-20	6.15-20
50	7.49-20	7.82-20	8.49-20	8.21-20	1.03-19	8.53-20	6.82-20
60	7.82-20	9.86-20	1.08-19	9.98-20	9.93-20	7.90-20	6.16-20
70	9.28-20	8.40-20	8.12-20	9.18-20	9.22-20	7.19-20	5.16-20
80	1.08-19	8.85-20	9.19-20	9.46-20	7.44-20	5.43-20	4.39-20
90	1.24-19	9.48-20	8.98-20	7.80-20	5.96-20	4.33-20	3.03-20
100	1.50-19	9.55-20	7.56-20	6.14-20	4.33-20	3.24-20	2.27-20
110	1.95-19	1.25-19	6.94-20	5.73-20	3.57-20	3.11-20	2.04-20
120	2.30-19	1.46-19	6.39-20	4.48-20	2.93-20	1.75-20	1.53-20
σ_I (cm^2)	2.42-18	1.70-18	1.12-18	9.68-19	8.17-19	6.09-19	4.51-19

* $2.13\text{-}18 = 2.13 \times 10^{-18}$.

feature with a sharp forward peak and a dip followed by a broad secondary maximum in the large angles. This feature is enhanced with the increase of the impact electron energy.

The angular distributions at intermediate and high energies are well interpreted by the Glauber calculations of Chang *et al.*[28] taking into account the contribution of three kinds of scattering mode. The sharp rise at forward scattering angles corresponds to the long range polarization effect. The broad secondary maximum at large angles comes from short range collisions with individual atomic nuclei (single scattering). The third is the double scattering contribution, in this energy region, which is shadowed by the polarization contribution and the single scattering contribution.

The DCS's at 10 eV and 80 eV are shown in Fig. 8 together with the previous experimental and theoretical results. The present results at 10 eV are in good agreement with the results of Trajmar *et al.*[27] in the forward scattering angles. The results of Linder and Schmidt[8] are in good agreement in shape but in magnitude about 20% smaller than the present results. It should be noted that the DCS's of Linder and Schmidt plotted here are the sum of the pure vibrational excitation ($v=0\rightarrow1$, $\Delta j=0$) and the vibrational rotational excitation ($v=0\rightarrow1, j=1\rightarrow3$). The present re-

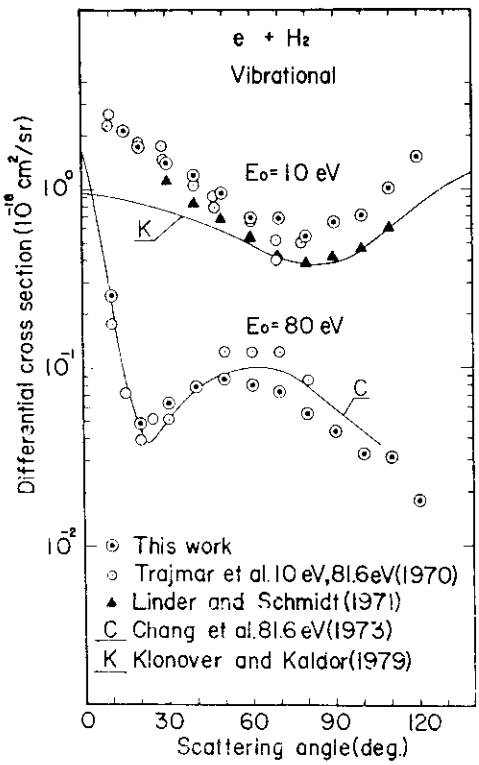

Fig. 8. Differential cross sections for vibrational excitation ($X^1\Sigma_g^+, v=0\rightarrow1$) as a function of scattering angle at 10 eV and 80 eV. Experimental results of Linder and Schmidt shown here are the sum of the pure vibrational ($v=0\rightarrow1, \Delta j=0$) and the vibrational rotational excitation ($v=0\rightarrow1, j=1\rightarrow3$).

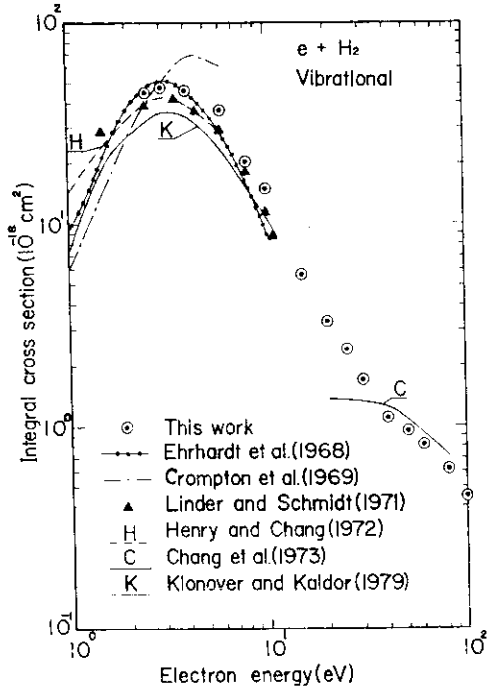

Fig. 9. Integral cross sections for vibrational excitation as a function of impact energy. The solid line C is presented by integrating the theoretical DCS's of Glauber calculations (ref. 28).

sults at 80 eV are in good agreement with the measurements of Trajmar *et al.* although the broad secondary maximum is slightly small in the present measurements. The present results are well reproduced by the calculations of Chang *et al.*[28] not only in shape but also in magnitude.

The integral cross sections are shown in Fig. 9 along with the experimental results of Ehrhardt *et al.*,[26] Crompton *et al.*,[2] and Linder and Schmidt. Also are shown the theoretical results of Henry and Chang,[30] Chang *et al.*,[28] and Klonover and Kaldor.[29] The cross sections obtained in the present measurements have a maximum at around 3 eV and decrease smoothly with the impact energies. There can be seen a small change in its slope at 40 eV. The present results are in good agreement with the measurements of Ehrhardt *et al.* at lower impact energies. However, the present results are higher than those of Ehrhardt *et al.*, and Linder and Schmidt between 6 eV to 10 eV.

§4. Summary

The elastic scattering cross sections obtained in the present measurements are in good agreement with the previous results within the experimental errors in the electron energy range observed. The elastic scattering cross sections are well predicted by the two center calculation and the close coupling calculation at low and intermediate energy regions. In the intermediate and high energy regions, the present results are well reproduced by the plane wave approximation including exchange and polarization. However, there are no complete theoretical calculations which predict the experimental results in the whole electron energy.

The vibrational DCS's show resonance structure at low electron energy region. At intermediate and high energy regions it shows a mixture of the two scattering modes, namely, the short range collision and the long range collision. The Glauber approximation gives good predictions of the DCS's at intermediate and high electron energy regions for $X^1\Sigma_g^+, v=0\rightarrow1$ excitation.

Acknowledgement

This work was partly supported by a Grant-in-Aid for Special Project Research from the Ministry of Education, Science and Culture. The authors thank Mr. K. Nishimura for his help in operating the computer. One of the authors (H. N.) thanks Dr. H. Tanaka and Dr. L. Boesten of Sophia University for their support of the computer programing.

References

1) D. E. Golden, H. W. Bandel and J. A. Salerno: Phys. Rev. **146** (1966) 40.
2) R. W. Crompton, D. K. Gibson and A. I. McIntosh: Aust. J. Phys. **22** (1969) 715.
3) A. G. Engelhardt and A. V. Phelps: Phys. Rev. **131** (1963) 2115.
4) S. Hara: J. Phys. Soc. Jpn. **27** (1969) 1009.
5) R. J. W. Henry and N. F. Lane: Phys. Rev. **183** (1969) 221.
6) D. G. Truhlar and M. A. Brandt: J. Chem. Phys. **65** (1976) 3092.
7) Burke: Phys. Rev. A **22** (1984) 92.
8) F. Linder and H. Schmidt: Z. Naturforsch. **26a** (1971) 1603.
9) S. Trajmar, D. G. Truhlar and J. K. Rice: J. Chem. Phys. **52** (1970) 4502.
10) S. P. Khare and P. Shobha: J. Phys. B **7** (1974) 420.
11) P. Gupta and S. P. Khare: J. Chem. Phys. **68** (1978) 2193.
12) P. K. Bhattacharyya, K. K. Goswami and A. S. Ghosh: Phys. Rev. A **18** (1978) 1865.
13) M. Fink, K. Jost and D. Herrmann: Phys. Rev. A **12** (1975) 1374.
14) B. van Wingerden, E. Weigold and F. J. Nygaard: J. Phys. B **10** (1977) 1345.
15) D. E. Golden, N. F. Lane, A. Temkin and E. Gerjuoy: Rev. Mod. Phys. **43** (1971) 642.
16) N. F. Lane: Rev. Mod. Phys. **52** (1980) 29.
17) S. Trajmar, D. F. Register and A. Chutjian: Phys. Rep. **97** (1983) 219.
18) C. R. Lloyd, P. J. O. Teubner, E. Weigold and B. R. Lewis: Phys. Rev. A **10** (1974) 175.
19) S. K. Srivastava, A. Chutjian and S. Trajmar: J. Chem. Phys. **63** (1975) 2659.
20) T. W. Shyn and W. E. Sharp: Phys. Rev. A **24** (1981) 1734.
21) J. Frust, M. Mahgerefteh and D. E. Golden: Phys. Rev. A **30** (1984) 2256.
22) J. W. McConkey and J. A. Preston: J. Phys. B **8** (1975) 63.
23) D. F. Register, S. Trajmar and S. K. Srivastava: Phys. Rev. A **21** (1980) 1134.
24) R. W. LaBahn and J. Callaway: Phys. Rev. A **2** (1970) 366.
25) D. E. Golden, J. Frust and M. Mahgerefteh: Phys. Rev. A **30** (1984) 1247.
26) H. Ehrhardt, L. Langhans, F. Linder and H. S. Taylor: Phys. Rev. **173** (1969) 222.
27) S. Trajmar, D. G. Truhlar, J. K. Rice and A. Kuppermann: J. Chem. Phys. **52** (1970) 4516.
28) T. N. Chang, R. T. Poe and P. Ray: Phys. Rev. Lett. **31** (1973) 1097.
29) A. Klonover and U. Kaldor: J. Phys. B **12** (1979) 323.
30) R. J. W. Henry and E. S. Chang: Phys. Rev. A **5** (1972) 276.
31) A. Chutjian: J. Chem. Phys. **61** (1974) 4279.
32) C. E. Kuyatt and J. A. Simpson: Rev. Sci. Instrum. **38** (1967) 103.
33) S. W. Jensen: Ph. D. Thesis, Univ. Calf., Riverside, 1978.
34) J. N. Bardsley and F. H. Read: Chem. Phys. Lett. **2** (1968) 333.
35) T. F. O'Malley and H. S. Taylor: Phys. Rev. **176** (1968) 207.